

Photosynth Res (2007) 94:291–297
DOI 10.1007/s11120-007-9177-x

RESEARCH ARTICLE

Time sequence of the damage to the acceptor and donor sides of photosystem II by UV-B radiation as evaluated by chlorophyll *a* fluorescence

Jack J. S. van Rensen · Wim J. Vredenberg ·
Gustavo C. Rodrigues

Received: 24 August 2006 / Accepted: 16 April 2007 / Published online: 8 May 2007
© Springer Science+Business Media B.V. 2007

Abstract The effects of ultraviolet-B (UV-B) radiation on photosystem II (PS II) were studied in leaves of *Chenopodium album*. After the treatment with UV-B the damage was estimated using chlorophyll *a* fluorescence techniques. Measurements of modulated fluorescence using a pulse amplitude modulated fluorometer revealed that the efficiency of photosystem II decreased both with increasing time of UV-B radiation and with increasing intensity of the UV-B. Fluorescence induction rise curves were analyzed using a mechanistic model of energy trapping. It appears that the damage by UV-B radiation occurs first at the acceptor side of photosystem II, and only later at the donor side.

Keywords *Chenopodium album* · Chlorophyll *a* fluorescence · Photosystem II · UV-B radiation · Photodamage · Photosynthesis

Abbreviations

Chl Chlorophyll
DCMU 3(3,4-dichlorophenyl)-1,1-dimethylurea
F_o Chlorophyll fluorescence at origin (O) in dark-adapted reaction centers with maximal photochemical quenching

F_m Maximum fluorescence at zero photochemical quenching
F_v Variable fluorescence
J, I Intermediate steps of chlorophyll fluorescence rise between O and P
OEC Oxygen evolving complex
P Fluorescence at peak
PAR Photosynthetically active radiation
PQ Plastoquinone
PS I Photosystem I
PS II Photosystem II
Q_A, Q_B Primary and secondary quinone electron acceptor of PSII, respectively
qN Non-photochemical quenching
qP Photochemical quenching
UV-B Ultraviolet-B radiation
Yz Redox-active tyrosine

Introduction

The solar spectrum that reaches the earth's surface includes wavelengths in the visible or photosynthetically active range (PAR, 400–700 nm), in the ultraviolet-A (UV-A, 320–400 nm), ultraviolet-B (UV-B, 280–320 nm) and in the ultraviolet-C (UV-C, 200–280 nm) ranges. While UV-C is totally absorbed by the atmosphere, ozone is the principal atmospheric attenuator of UV-B radiation (Cockell and Horneck 2001). The depletion of ozone by the emission into the atmosphere of man-made chlorine- and bromine-containing compounds has been correlated with an increase in the background level of UV-B radiation.

J. J. S. van Rensen (✉) · W. J. Vredenberg ·
G. C. Rodrigues
Laboratory of Plant Physiology, Wageningen University
and Research Center, Arboretumlaan 4, Wageningen 6703 BD,
The Netherlands
e-mail: Jack.VanRensen@wur.nl

Present Address:
G. C. Rodrigues
Embrapa-Cerrados, Planaltina, DF, Brazil

UV-B radiation can affect a multitude of physiological and morphological plant processes that ultimately can lead to inhibition of growth and reproduction (Jansen et al. 1998). Potential molecular targets for direct UV-B damage via photomodification or photosensitization include nucleotides, proteins, lipids and pigments (Jordan 2002). Besides direct macromolecular damage, UV-B can also induce specific signal transduction pathways and changes in gene expression that stimulates acclimation and repair processes (Holl  sy 2002; Brosch   and Strid 2003).

The photosynthetic process can be affected by UV-B radiation at different levels, including alterations in plant and leaf morphology that decreases light interception (Jansen 2002), changes in stomatal function that limit the availability of CO₂, changes in photosynthetic pigments (Strid and Porra 1992), on the expression of photosynthetic genes and on enzymes of the carbon fixation pathway. However, it is the effects of UV-B radiation on light harvesting and primary photochemical reactions of photosynthetic membranes, particularly on the Photosystem II (PS II) reaction center, which has attracted much attention and study (Vass 1997; Vass et al. 2005).

PS II is one of the reaction centers that, together with the cytochrome b₆f complex, the photosystem I (PS I) reaction center, and the ATP-synthase, forms the electron transport chain that drives energy transduction in the thylakoid membranes of oxygenic eukaryotes. The photochemical core of PS II is formed by the D1/D2 heterodimer, where the redox electron carriers and cofactors of electron transport are bound. Light absorbed by the antenna system of PS II induces the excitation of a special reaction center chlorophyll (P680), which is photo-oxidized on the first electron transfer reaction of PS II, with a pheophytin molecule (Pheo) acting as the primary electron acceptor and the formation of a radical pair state (P680⁺Pheo[−]). This radical pair state is “stabilized” at the reducing (acceptor) side of PS II by the electron transfer from Pheo[−] to a primary D2-bound quinone electron acceptor (Q_A) and then to the secondary D1-bound quinone acceptor (Q_B), which, upon accumulation of two reducing equivalents, and becoming protonated to plastoquinol, dissociates from the reaction center. At the oxidizing (donor) side of PS II, P680⁺ is reduced by a redox-active tyrosine residue of D1 (Y_Z) which acts as an electron transfer intermediate between P680⁺ and the oxygen-evolving complex (OEC), the metalloenzyme system composed of a cluster of four Mn ions and inorganic cofactors (Ca²⁺ and Cl[−]) that oxidizes water into molecular oxygen. Accordingly, the consecutive photochemical formation of the primary radical pair P680⁺Pheo[−] by light absorption and the reduction of P680⁺ forming the radical Y_Z⁺ drives the sequential four-step oxidation of the OEC inducing the S-state transitions and ultimately the splitting of the water molecule. For detailed

reviews on oxygen evolution and PS II structure and function see, Diner and Babcock (1996), Xiong et al. (1998), and Van Rensen and Curwiel (2000).

From the above brief description of the PS II components and the potential molecular targets of UV-B radiation, it is clear that several components of PS II could be directly affected, as actually has been observed (Vass et al. 1996). Several studies, most of them in vitro, have shown that UV-B can inhibit PS II electron transport by damage to the quinone electron acceptors’ redox function (Rodrigues et al. 2006), to Y_Z function, to the OEC, and to the D1 protein. It should be noted that the time-sequence of events that ultimately leads to inactivation of PS II function is not completely clear, as it might involve a direct destruction or impairment of the absorbing molecule, modification of the protein environment to which these redox components are bound as well as a process of energy transfer by the sensitizer species to the damaged site (Vass 1997).

The time sequence of damage to acceptor and donor sides of PS II, respectively has never been measured in a single experiment. In this work, we have studied the effect of UV-B radiation on the function of PS II in leaves of *Chenopodium album* using both steady-state (light-adapted) fluorescence and the time-resolved fast Chl-*a* fluorescence induction curve. For a review on Chl-*a* fluorescence, see Govindjee (1995). The results were analyzed based on a mechanistic model of energy trapping and electron transport of PS II (Vredenberg 2000). It appears that damage to the acceptor side of PS II occurs first, and that only later the donor side becomes affected.

Materials and methods

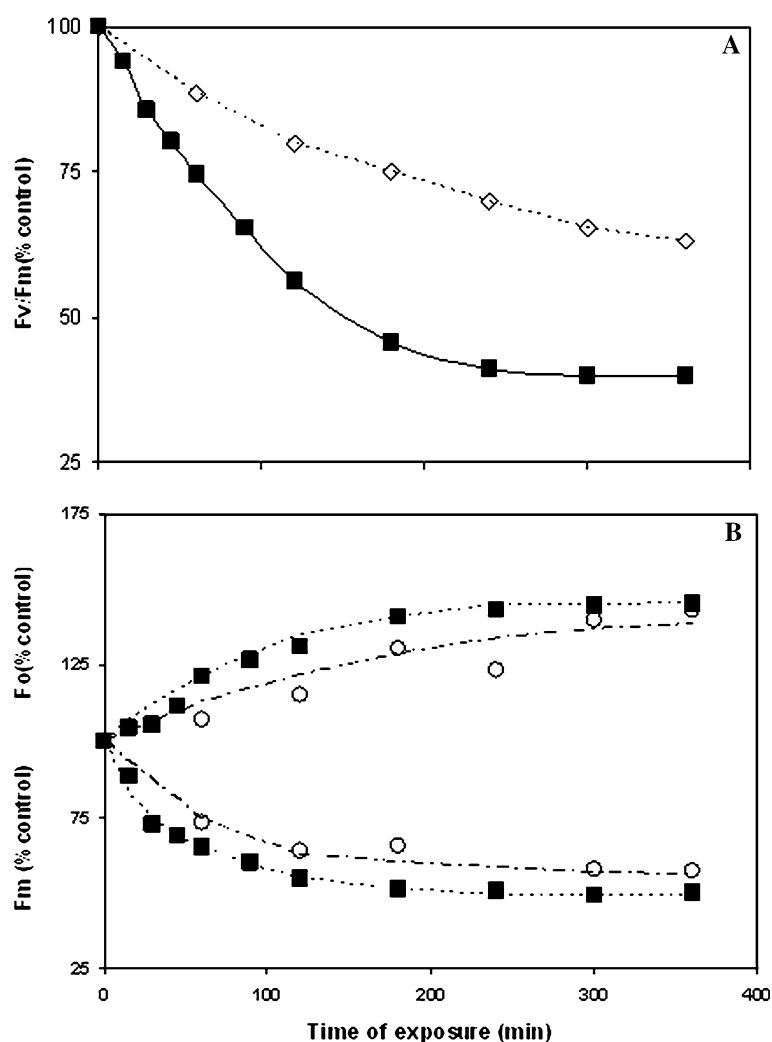
Plant growth

Plants of *Chenopodium album* L. were grown as described earlier (Rodrigues et al. 2006). After around 28 days the plants were transferred to a growth cabinet with a constant temperature of 20°C, 70% relative humidity and a PAR level of 60 μmol m^{−2} s^{−1}. The plants were watered daily and after 10–14 days the sampling of leaves for the UV exposure treatments started. Several different batches of plants were used and no significant difference could be detected when comparing results from experiments replicated with plants with similar ages but from different batches.

UV-B radiation treatments

The plant material used for the exposure to UV light was either fully developed detached leaves or leaf discs (0.6 cm²) floating on petri-dishes filled with demineralized

Fig. 1 Effect of UV-B radiation of variable duration on F_o , F_m , and the F_v/F_m ratio in leaf discs. The UV-B radiation level was 720 (■), or 150 (○) $\mu\text{mol m}^{-2} \text{s}^{-1}$, respectively (PAR level was zero); control samples were kept in darkness. Each value is the mean of four measurements and the bars indicate \pm S.D.; bars not shown are within the symbols



water with the abaxial leaf surface exposed to the radiation. The control samples were either kept in the darkness or exposed to white light (PAR). In some experiments leaves were vacuum infiltrated with 3-(3,4-dichlorophenyl)-1, 1-dimethylurea (DCMU) in 0.5% ethanol before being exposed to UV-B, with the controls infiltrated with a 0.5% ethanol solution.

UV-B irradiations were performed using a Vilber Lourmat lamp with filter (VL-115M, Marne-la-Vallée, France). This lamp has a peak emission at 312 nm. UV-B irradiance was measured with an optometer (United Detector Technology Inc, Baltimore, USA) equipped with a probe specific for UV radiation.

Chlorophyll *a* fluorescence measurements

Measurements of Chl-*a* fluorescence were performed at room temperature on leaf samples that had been dark adapted for 1 h after the exposure to UV-B radiation, unless otherwise stated. Steady-state Chl-*a* fluorescence

was measured with a pulse-amplitude fluorometer (PAM 101–103, Walz Inc., Effeltrich, Germany). A weak modulated measuring light (1.6 kHz, 650 nm) was used for the determination of the minimal fluorescence level F_o , followed by a 1 s pulse of saturating light ($5,500 \mu\text{mol m}^{-2} \text{s}^{-1}$) for the measurement of the maximum fluorescence level F_m . The leaf was then irradiated with a fixed or increasing level of actinic PAR and, at each level, we measured the steady state light-adapted fluorescence (F_o'), the maximum fluorescence of a light-adapted state (F_m') induced by a saturating light pulse superimposed on the actinic light, and after removing the actinic light and the application during 10 s of far-red light ($6 \mu\text{mol m}^{-2} \text{s}^{-1}$, 720 nm), the minimum fluorescence of a light-adapted state (F_o''). During the saturating pulses the modulation of the measuring light was automatically changed to 100 kHz. Several fluorescence parameters were calculated from the measured fluorescence levels (Schreiber et al. 1986; Genty et al. 1989; Van Kooten and Snel 1990): the potential photochemical efficiency (quantum yield) of PS II, expressed as the ratio

Fig. 2 Effects of 6 h irradiation, at various levels, of detached leaves on some fluorescence parameters. CO is control; control is white light (PAR); UV-B is given by the Vilber lamp (zero PAR). Each value is the average of 4 measurements and the bars indicate \pm S.D.; bars not shown are within the symbols

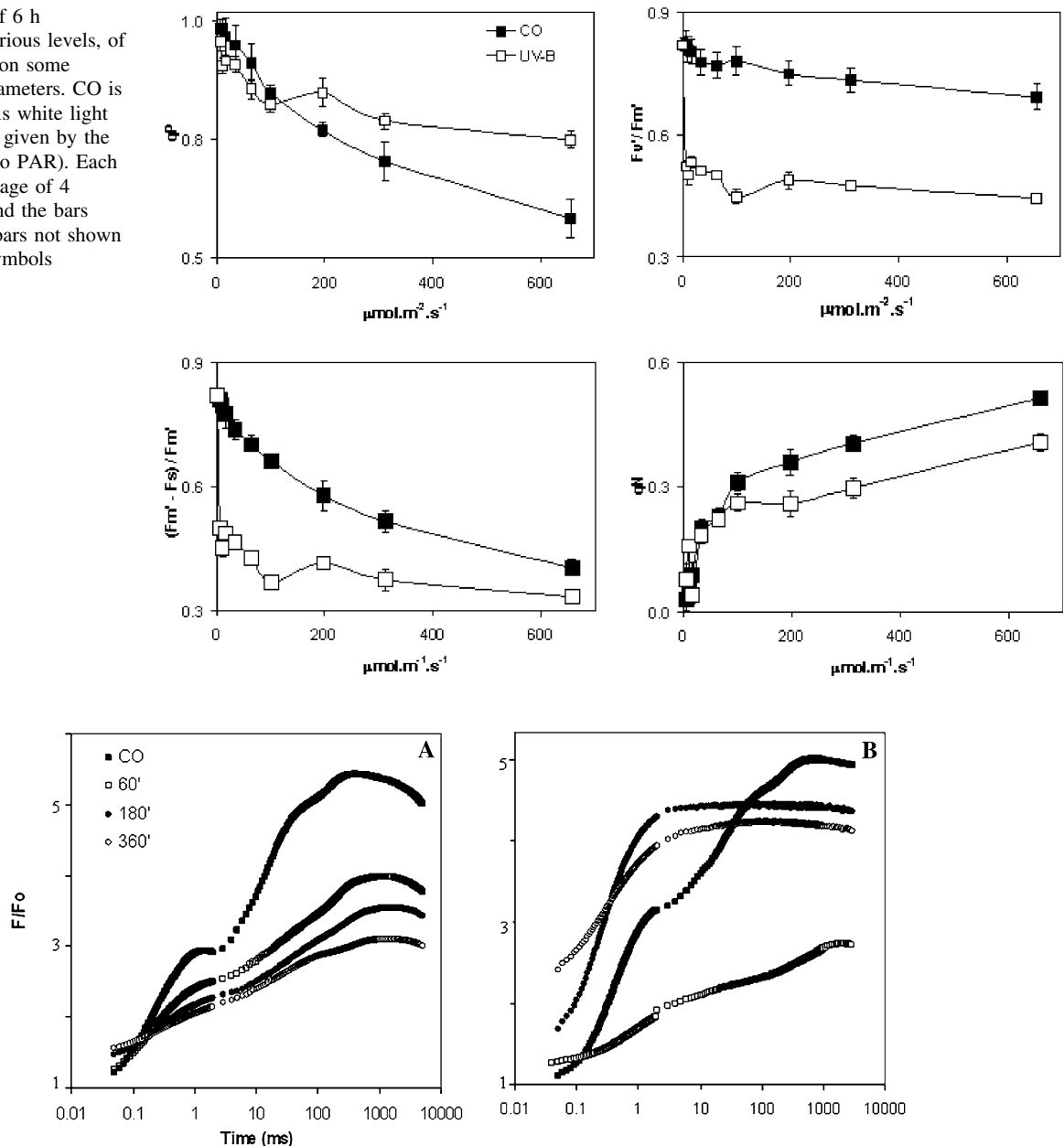


Fig. 3 Fluorescence induction curves after various treatments of leaves. **(A)** Fluorescence transients after 0, 60, 180, and 360 min irradiation with UV-B light at $150 \mu\text{mol}\cdot\text{m}^{-2}\cdot\text{s}^{-1}$. (PAR is zero). **(B)** ■, After infiltration with 0.5% ethanol (CO is control), no UV-B; ●, after infiltration with 10^{-5} M DCMU in 0.5% ethanol, no UV-B; □,

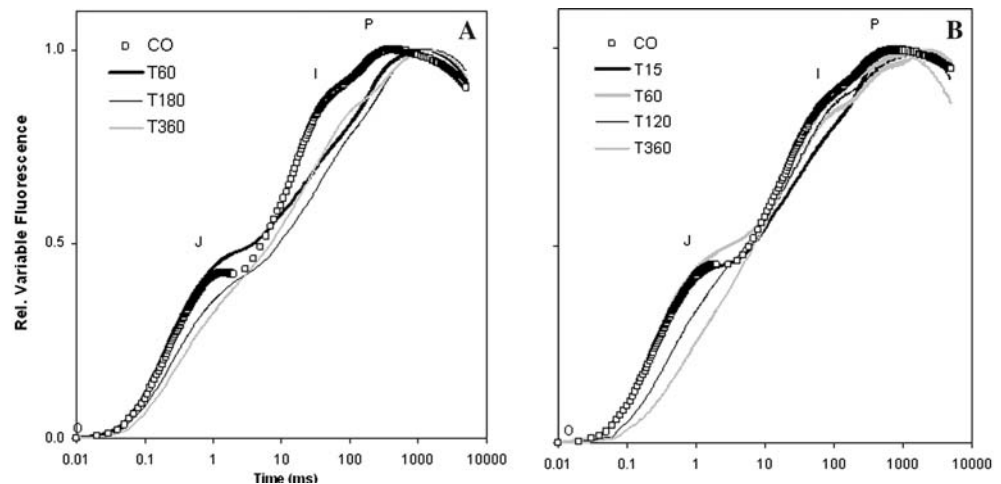
after infiltration with 0.5% ethanol and 6 h irradiation with $150 \mu\text{mol}\cdot\text{m}^{-2}\cdot\text{s}^{-1}$ UV-B light; ○, after infiltration with 10^{-5} M DCMU in 0.5% ethanol and 6 h irradiation with UV-B. Each curve is the average of three measurements

F_v/F_m with $F_v = F_m - F_o$; the coefficient of photochemical quenching, qP , given by $(F_m' - F_s)/F_v'$ with $F_v' = F_m' - F_o'$; the efficiency of excitation energy capture by open PS II reaction centers, F_v'/F_m' ; and non-photochemical quenching, qN , given by $1 - (F_m' - F_o')/(F_m - F_o)$ (Walters and Horton 1991).

The fast Chl-*a* fluorescence rise was measured with the Plant Efficiency Analyser (PEA, Hansatech Ltd, Norfolk, UK). Leaf samples were excited with a saturating pulse of

red light (peak at 650 nm, $3,500 \mu\text{mol}\cdot\text{m}^{-2}\cdot\text{s}^{-1}$) and the fluorescence signal recorded at an acquisition interval of 10 μs in the first 2 ms of excitation (for more details on this instrument see Strasser et al. (1995, 2000): a model describing discrete steps of excitation energy and electron transfer associated with PS II was published by Zhu et al. (2005). Due to the limiting response time of the fluorescence detector in the time region below 50 μs , the F_o level was taken as the model-calculated (see below) fluorescence

Fig. 4 Relative variable fluorescence measured after illumination of leaves during various times (T , in min) with UV-B light at 150 (A) or 720 $\mu\text{mol m}^{-2} \text{s}^{-1}$ (B); PAR is zero. CO is control. Each curve is the average of three (A) or four (B) measurements



level at 10 μs . This procedure gave similar results to the method of extrapolation as proposed by Vredenberg (2000). The fast Chl-*a* fluorescence rise is plotted in a log-time scale either as the absolute measured values or as the relative variable fluorescence (rF_v), calculated as $(F_m - F_t)/(F_m - F_0)$, with F_t as the fluorescence level at any time.

Modeling and interpretation of fast Chlorophyll *a* fluorescence rise

The fast Chl-*a* fluorescence rise curve was modeled according to Vredenberg et al. (2001). The mathematical formulation is based on a three-state model of energy trapping and fluorescence (Vredenberg 2000) and equates the polyphasic fluorescence rise upon a saturating pulse of light to a multi-state transfer pattern of the PS II reaction center.

Results and discussion

Exposure of the leaves to UV-B radiation caused an increase of F_0 and a decrease of F_m (Fig. 1B), resulting in a decrease of the F_v/F_m value (Fig. 1A). Using a lower intensity of UV-B radiation on grape leaves, Pfündel (2003) also found a decrease of F_m . However, in his experiments, the F_0 first decreased with time, and only increased after about 3 h. The increase of the F_0 indicates an increase in the amount of Q_B -nonreducing centers; the decrease of the F_v/F_m value indicates that UV-B has a strong damaging effect on the functioning of PS II.

Illumination with white light during 6 h decreased the photochemical quenching qP from 1.0 at the lowest intensity to a value of 0.58 at 656 $\mu\text{mol m}^{-2} \text{s}^{-1}$ (Fig. 2). Curwiel et al. (1993), using the same plant material, reported a decrease to about 0.80 after illumination at about

500 $\mu\text{mol m}^{-2} \text{s}^{-1}$. Up to 100 $\mu\text{mol m}^{-2} \text{s}^{-1}$, irradiation with UV-B has a stronger effect on qP than white light; at 200 $\mu\text{mol m}^{-2} \text{s}^{-1}$ and higher, the effect of UV-B is smaller. The efficiency of excitation energy capture by open PS II reaction centers, F_v'/F_m' , was already decreased strongly after 6 h at 5.4 $\mu\text{mol m}^{-2} \text{s}^{-1}$ of UV-B, while the effect of white light is much smaller; comparable results were found for the quantum yield of PS II given by $(F_m' - F_s)/F_m'$. The non-photochemical qN increased from 0 at the lowest intensities to 0.51 (white light) and 0.41 (UV-B) at the highest irradiation levels. Curwiel et al. (1993) reported a value of about 0.6 after illumination with white light at about 550 $\mu\text{mol m}^{-2} \text{s}^{-1}$.

Measurements of Chl-*a* fluorescence transients of intact leaves with the PEA fluorometer are presented in Fig. 3. In Fig. 3A the effects of 0, 1, 3, and 6 h irradiation with the Vilber UV-B lamp at 150 $\mu\text{mol m}^{-2} \text{s}^{-1}$ are illustrated. Also in these measurements, the most obvious effects of UV-B are an increase of the F_0 level and a decrease in F_m . After infiltration with water (plus 0.5% ethanol) the effects of UV-B appear the same (compare in Fig. 3B, \square with \blacksquare). Compared with infiltration with water, infiltration with DCMU (\bullet) causes a much higher F_0 level, and a faster increase to the J-P level; irradiation with UV-B after DCMU-infiltration (\circ) causes a still higher F_0 level and a slower increase to the J-P level. Comparable results were found using another PS II-inhibiting herbicide, atrazine (not shown). The higher F_0 level indicates an increased amount of Q_B -nonreducing centers. Apart from the F_0 level, the differences between the curves before and after UV-B treatment are much smaller in the presence of DCMU. This may be related with the finding by Jansen et al. (1993) that PS II-inhibitors like DCMU, which replace Q_B from its niche on the D1 protein, inhibit UV-B-driven D1 degradation.

To study the kinetics of the various parts of the transients, induction curves were normalized (Fig. 4). While

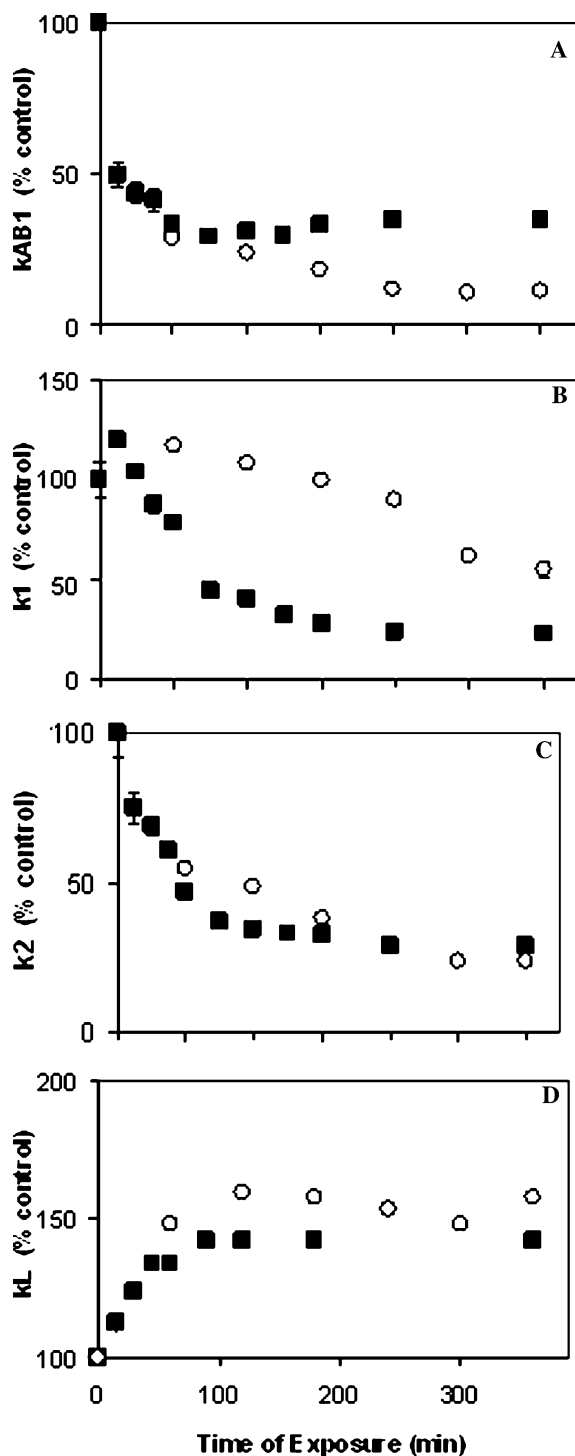


Fig. 5 Rate constants of some reactions involved in the photochemical trapping in the reaction center of PS II, calculated using the Three-State Trapping Model of PS II (Vredenberg 2000). Curves like those presented in Fig. 5 were taken as a source for the calculations; these curves were measured after various times of irradiation with the Vilber lamp at $150 \mu\text{mol m}^{-2} \text{s}^{-1}$ (○) or $720 \mu\text{mol m}^{-2} \text{s}^{-1}$ (■); PAR was zero. Average of four measurements and the bars indicate \pm S.D.; bars not shown are within the symbols

the level of the J transient increases a little after 60 min UV-B, it decreases clearly after 180 and 360 min UV-B; the kinetics of the O-J increase become lower after UV-B irradiation. In all cases the level of the I transient decreases and the kinetics of the J-(I)P rise decreases. From curves like those in Fig. 4, rate constants of reactions involved in the photochemical trapping in the reaction center of PS II were calculated using the Three-State Trapping Model of PS II (Vredenberg 2000; Vredenberg et al. 2001). The rate constants for Q_A^- oxidation by Q_B (k_{AB1}) decreased very fast, both at 150 and $720 \mu\text{mol m}^{-2} \text{s}^{-1}$; it is down to about 50% of control already after 15 min UV-B irradiation (Fig. 5A). The rate constant for Q_A^- oxidation by Q_B^- (k_{AB2}) was down to 5% of control, already after 15 min UV-B (not shown). This indicates that UV-B irradiation has a fast action on the reducing side of PS II. The rate constants for Yz^+ reduction by the OEC in S_1 and S_2 (k_1 and k_2 in Fig. 5B and C, respectively), were also affected, but much slower. From this we conclude that the damage by UV-B starts at the reducing side, and affects the donor side later. In Fig. 5D it is illustrated that k_L (excitation rate) increases by UV-B irradiation. This indicates that UV-B radiation decreases the antenna size, or that a lower number of open reaction centers is available after UV-B treatment.

As may be concluded from the results presented in Fig. 5, UV-B radiation affects rate constants of reactions at both the acceptor and donor sides of PS II. With respect to the acceptor side, Rodrigues et al. (2006) reported that Q_A^- is a photosensitizer for UV-B radiation; absorption of UV-B by this semiquinone radical initiates reactions leading to damage to PS II. The group of Vass, most often using isolated plant preparations, has reported several times on the effect of UV-B radiation on the donor side of PS II. In a recent paper (Szilard et al. 2006), they describe a model where UV-B-induced inhibition of water oxidation is caused either by direct absorption within the catalytic manganese cluster or by damaging intermediates of the water oxidation process.

Vass et al. (1996) measured the effects of UV-B radiation on the OEC, the $Q_A\text{Fe}^{2+}$ complex, the redox-active tyrosines, and the D1 protein in isolated spinach PS II membrane particles. While all these functions were affected, the OEC appeared to be the most sensitive; the authors concluded that the primary damage by UV-B occurs at the OEC, and that modification and/or inactivation of tyrosine and the quinone acceptor complex are subsequent events. Our work confirms that UV-B radiation affects both acceptor and donor sides of PS II. However, our analysis leads to the conclusion that the acceptor side of PS II is affected first and the donor side later. This

different conclusion may be caused by the different material and methods of the two works. Vass et al. (1996) used PS II particle membranes, while in our work intact leaves were measured. Furthermore, Vass et al. (1996) measured the effect of UV-B separately on the various PS II functions, while we calculated the effects of UV-B from one single measurement.

Acknowledgement This work has been supported in part by a scholarship from the Brazilian Agricultural Research Corporation (Embrapa) to G.C.R.

References

- Brosché M, Strid A (2003) Molecular events following perception of ultraviolet-B radiation by plants. *Physiol Plant* 117:1–10
- Cockell CS, Horneck G (2001) The history of the UV radiation climate of the earth—theoretical and space-based observations. *Photochem Photobiol* 73:447–451
- Curwiel VB, Schansker G, De Vos O, Van Rensen JJS (1993) Comparison of photosynthetic activity in triazine-resistant and susceptible biotypes of *Chenopodium album*. *Z Naturforsch* 48c:278–282
- Diner BA, Babcock GT (1996) Structure, dynamics, and energy conversion efficiency in photosystem II. In: Ort DR, Yocum CF (eds) *Oxygenic photosynthesis: the light reaction*, Kluwer, Dordrecht, The Netherlands, pp 213–247
- Genty B, Briantais J-M, Baker NR (1989) The relationship between quantum yield of photosynthetic electron transport and quenching of chlorophyll fluorescence. *Biochim Biophys Acta* 990:87–92
- Govindjee (1995) Sixty-three years since Kautsky: chlorophyll *a* fluorescence. *Aust J Plant Physiol* 22:131–160
- Hollósy F (2002) Effects of ultraviolet radiation on plant cells. *Micron* 33:179–197
- Jansen MAK (2002) Ultraviolet-B radiation effects on plants: induction of morphogenic responses. *Physiol Plant* 116:423–429
- Jansen MAK, Depka B, Trebst A, Edelman M (1993) Engagement of specific sites in the plastoquinone niche regulates degradation of the D1 protein in photosystem II. *J Biol Chem* 268:21246–21252
- Jansen MAK, Gaba V, Greenberg BM (1998) Higher plants and UV-B radiation: balancing damage, repair and acclimation. *Trends Plant Sci* 3:131–135
- Jordan BR (2002) Molecular response of plant cells to UV-B stress. *Funct Plant Biol* 29:909–916
- Pfündel EE (2003) Action of UV and visible radiation on chlorophyll fluorescence from dark-adapted grape leaves (*Vitis vinifera* L.). *Photosynth Res* 75:29–39
- Rodrigues GC, Jansen MAK, Van den Noort ME, Van Rensen JJS (2006) Evidence for the semireduced primary quinone electron acceptor of photosystem II being a photosensitizer for UVB damage to the photosynthetic apparatus. *Plant Sci* 170:283–290
- Schreiber U, Schliwa U, Bilger W (1986) Continuous reading of photochemical and non-photochemical chlorophyll fluorescence quenching with a new type of modulation fluorometer. *Photosynth Res* 10:51–62
- Strasser RJ, Srivastava A, Govindjee (1995) Polyphasic chlorophyll *a* fluorescence transient in plants and cyanobacteria. *Photochem Photobiol* 61:32–42
- Strasser RJ, Srivastava A, Tsimilli-Michael M (2000) The fluorescence transient as a tool to characterize and screen photosynthetic samples. In: Mohanty P, Yunus M, Pathre U (eds) *Probing photosynthesis: Mechanism, Regulation and Adaptation*. Taylor and Francis, London, pp 445–480
- Strid A, Porra RJ (1992) Alterations in pigment content in leaves of *Pisum sativum* after exposure to supplementary UVB. *Plant Cell Physiol* 33:1015–1023
- Szilard A, Sass L, Deak Z, Vass I (2006) The sensitivity of photosystem II to damage by UV-B radiation depends on the oxidation state of the water-splitting complex. *Biochim Biophys Acta* doi: 10.1016/j.bbabi.2006.11.020
- Van Kooten O, Snel JFH (1990) The use of chlorophyll fluorescence nomenclature in plant stress physiology. *Photosynth Res* 25:147–150
- Van Rensen JJS, Curwiel VB (2000) Multiple functions of photosystem II. *Indian J Biochem Biophys* 37:377–382
- Vass I (1997) Adverse effects of UV-B light on the structure and function of the photosynthetic apparatus. In: Pessarakli M (ed) *Handbook of photosynthesis*, Marcel Dekker Inc, New York, pp 931–949
- Vass I, Sass L, Spetea C, Bakou A, Ghanotakis DF, Petrouleas V (1996) UV-B-induced inhibition of photosystem II electron transport studied by EPR and chlorophyll fluorescence. Impairment of donor and acceptor side components. *Biochemistry* 35:8964–8973
- Vass I, Szilard A, Sicora C (2005) Adverse effects of UV-B light on the structure and function of the photosynthetic apparatus. In: Pessarakli M (ed) *Handbook of photosynthesis* 2nd ed. Marcel Dekker Inc, New York, pp 827–843
- Vredenberg WJ (2000) A 3-state model for energy trapping and chlorophyll fluorescence in Photosystem II incorporating radical pair recombination. *Biophys J* 79:25–38
- Vredenberg WJ, Rodrigues GC, Van Rensen JJS (2001) A quantitative analysis of the chlorophyll fluorescence induction in terms of electron transfer rates at donor and acceptor sides of photosystem II. In: *PS2001 Proceedings 12th Int. Congress on photosynthesis*, CSIRO Publishing, Melbourne (CD-ROM)
- Walters RG, Horton P (1991) Resolution of components of non-photochemical chlorophyll fluorescence quenching in barley leaves. *Photosynth Res* 27:121–133
- Xiong J, Subramaniam S, Govindjee (1998) A knowledge-based three dimensional model of the Photosystem II reaction center of *Chlamydomonas reinhardtii*. *Photosynth Res* 56:229–254
- Zhu X, Govindjee, Baker NR, DeSturle E, Ort DR, Long SP (2005) Chlorophyll *a* fluorescence induction kinetics in leaves predicted from a model describing each discrete step of excitation energy and electron transfer associated with photosystem II. *Planta* 223:14–133